

Electronic Structure of Exciplexes and the Role of Local Triplet States on Efficiency of Thermally Activated Delayed Fluorescence

Marian Chapran, Ihor Sahalianov, Nataliya N. Karaush-Karmazin, Gabriela Wiosna-Salyga, Ireneusz Glowacki, Beata Luszczynska, Piotr Pander,* and Glib V. Baryshnikov*

Cite This: *ACS Appl. Electron. Mater.* 2023, 5, 1489–1501

Read Online

ACCESS |

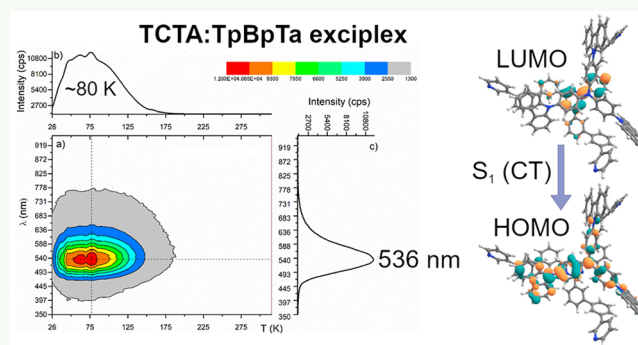
Metrics & More

Article Recommendations

Supporting Information

ABSTRACT: In this work, we present an investigation of the electronic states in a series of thermally activated delayed fluorescence (TADF) exciplexes formed with the popular electron-transport compound TpBpTa and hole-transporting TCTA, TAPC, TPD10, TPD, and NPB. We rationalize the photophysical behavior of exciplexes by using computational methods and demonstrate that the reason for the commonly observed temporal red shift in the time-resolved spectra is related to the distribution of molecular conformations, thus CT energy, in film. We also use spectrally resolved thermoluminescence (SRTL) measurements to give insight into the trapping phenomena in exciplex blends. The results demonstrate that trapped charge carriers in the majority of studied exciplexes recombine through the luminescent intermolecular CT state. In addition, we report OLED devices using the said exciplexes in the emissive layer. The best performance is obtained with the TCTA:TpBpTa and TAPC:TpBpTa exciplexes showing maximum external quantum efficiencies (EQEs) of 8.8% and 7.2%, respectively.

KEYWORDS: exciplex, thermally activated delayed fluorescence, TADF, OLED, charge-trapping



INTRODUCTION

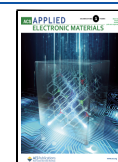
In past decades, organic light-emitting diode (OLED) technology has shown an intense and fast development and has been applied commercially in lighting and luminescent displays. The light-emitting layer plays a crucial role in OLEDs, where charge carriers injected into the device recombine, producing singlet and triplet excited states at a ratio of 1:3.¹ To achieve 100% internal quantum efficiency of electroluminescence, the normally dark triplet excited states must be harvested. This can be achieved by room temperature phosphorescence in organometallic complexes² or by thermally activated delayed fluorescence (TADF).³ Purely organic emitters exhibiting TADF can display competitive efficiency relative to more conventional metal-based luminophores and are often preferred, as they do not require precious metals in the structure. TADF, also known as E-type delayed fluorescence, involves up-conversion of triplet excitons into the singlet state.⁴ An important factor in efficient TADF is a small singlet–triplet energy gap (ΔE_{ST}).⁵ The simplest way to reduce the ΔE_{ST} is by using donor (D) and acceptor (A) groups in the molecular structure leading to *intra*-molecular excited charge-transfer (CT) states.⁶ Similar, but *inter*-molecular excited CT states can be observed in blends of D and A, also known as exciplexes.⁷ Although exciplexes have been known since the 1960s,⁸ they have only gained significant

attention as emitters in OLED in the past 20 years. Exciplexes have initially been considered as an undesirable quenching mechanism in OLEDs,⁹ but since Goushi et al. have demonstrated TADF in a blend of 4,4',4''-tris[3-methylphenyl-(phenyl)amino] triphenylamine (m-MTDATA) with 2,8-bis(diphenylphosphoryl)dibenzo[b,d]thiophene (PPT)¹⁰ and m-MTDATA with 2-(biphenyl-4-yl)-5-(4-*tert*-butylphenyl)-1,3,4-oxadiazole (*t*-Bu-PBD),⁷ they became a point of interest as potentially highly efficient OLED luminophores. Exciplexes have made enormous progress since, being used as components of OLEDs, organic solar cells,^{11,12} organic field-effect transistors,^{13,12,14} light-emitting electrochemical cells,^{15,16} and others. Exciplex OLEDs have already reached efficiencies comparable to those of molecular state-of-the-art TADF emitters with an external quantum efficiency (EQE) at 20% for blue, 24% for green, 10% for red, and 1% for the near-infrared regions of the spectrum.^{17–19} Besides their highly efficient luminescence, exciplexes serve as excellent hosts in

Received: November 7, 2022

Accepted: February 7, 2023

Published: February 20, 2023



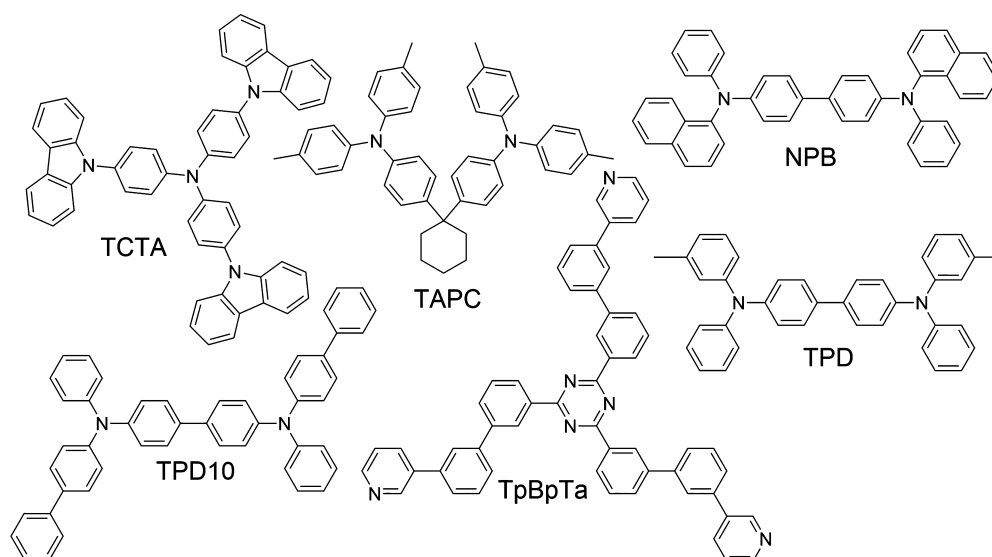


Figure 1. Chemical structure of exciplex forming materials used in this work.

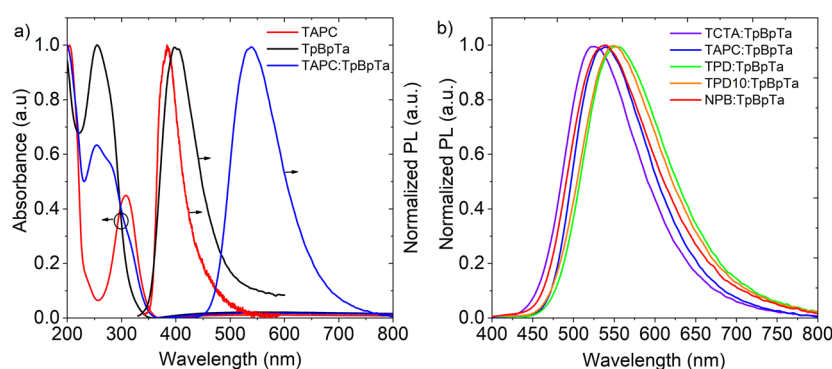


Figure 2. (a) Normalized absorption spectra in the film of TAPC, TpBpTa, and their blends; (b) normalized photoluminescence (PL) spectra of exciplex blends in films.

phosphorescent, TADF, and hyperfluorescent OLEDs.²⁰ A typical approach to achieving exciplex luminescence is to mix unipolar electron-donating (D) and electron-accepting molecules (A) or to combine a D–A type bipolar material with A or D molecules.²¹ As shown earlier,²² exciplex systems require a specific configuration between the HOMO and LUMO of the D and A to form. Relatively high triplet energy of the counterparts is necessary to yield TADF, while efficient charge transport is vital in devices.

Luminescent efficiency of exciplexes is often limited by nonradiative processes.²³ However, it has been shown that accelerating the harvesting of triplet excitons facilitates reducing the detrimental effect of nonradiative pathways, leading to increased OLED efficiencies. This promotion of triplet harvesting can be achieved by enhancing spin–orbit coupling between singlet and triplet states^{24,25} or by increasing the number of RISC channels^{17,26}—the latter with more success so far. The high efficiency of exciplexes has been achieved by using a conventional TADF emitter as either the D or A or by using three-component systems.^{17,27} Nevertheless, simple D–A systems remain more useful for an understanding of the intrinsic behavior of exciplexes.

One of the somewhat more obscure features of TADF exciplexes is the actual mechanism of the reverse intersystem crossing (RISC). It is well-known that an efficient RISC in a

D–A system requires a third, triplet state as a mediator given that the emissive ¹CT state is accompanied by a close lying ³CT of virtually the same orbital topology.^{28–30} Since spin–orbit coupling matrix element $\langle {}^3\text{CT} | H_{\text{SO}} | {}^1\text{CT} \rangle \approx 0$ due to the practically same orbital geometry of both states, the third state of a different topology is necessary for RISC to be efficient—it is often the local triplet state of D or A, ³LE_{D/A}.

In our work, we aim to study exciplex systems either in which the ³LE is an obvious mediator state or in which the role of the local triplet state is somewhat less clear, suggesting that something other than local states must be involved in the RISC mechanism. We have selected a group of five exciplexes with a similar steady state photoluminescence to study the effects of the relative configuration of the ¹CT/³CT and ³LE on exciplex TADF. Using in depth photophysical and computational techniques, we demonstrate that upper CT states may serve as substitute mediator states in the absence of obvious ³LE states near the S₁/T₁ manifolds.

Green OLEDs based on investigated charge transfer systems yielded electro-optical performance in accordance with photophysical and theoretical studies. Additionally, charge-trapping and the radiative recombination phenomena of exciplex emitters have been investigated by spectrally resolved thermoluminescence (SRTL) techniques.^{31,32}

RESULTS AND DISCUSSION

Photophysics. Figure 1 presents the chemical structures of commercially available OLED fabrication materials used in this study. We have selected five donor molecules with similar ionization energy: TCTA {tris(4-carbazoyl-9-ylphenyl)amine}, TAPC {4,4'-cyclohexylidenebis[N,N-bis(4-methylphenyl)benzenamine]}, TPD10 {N4,N4'-di(biphenyl-4-yl)-N4,N4'-diphenylbiphenyl-4,4'-diamine}, TPD {N,N'-bis(3-methylphenyl)-N,N'-diphenylbenzidine}, and NPB {N,N'-di(1-naphthyl)-N,N'-diphenyl-(1,1'-biphenyl)-4,4'-diamine}. Formation of the exciplex CT state occurs through electron donation by the excited state of the donor D^* to the A molecule.^{33,34} Generally speaking, triazine-based acceptors have been popular exciplex forming materials due to their electron-deficient structure.^{35–37} We have selected a molecule from this group as an electron acceptor for the study: TpBpTa {2,4,6-tris(3'-(pyridin-3-yl)-[1,1'-biphenyl]-3-yl)-1,3,5-triazine}. TpBpTa has a high molecular weight, high triplet energy, propeller-shaped structure, and high electron mobility and thus is perfectly suited for the study.^{11,38} To the best of our knowledge, the presented exciplexes have not been reported previously, except for the TCTA:TpBpTa blend.³⁹

Normalized absorption and photoluminescence spectra of TAPC, TpBpTa, and their blends are presented in Figure 2a. Absorption spectra of the blend are a simple superposition of individual components, indicating no aggregation or formation of CT in the ground state. At the same time, the PL spectrum of the TAPC:TpBpTa exciplex blend is visibly red-shifted compared to PL spectra of TAPC and TpBpTa individual films.^{33,40} Corresponding behavior was observed also in all of the other blends (Figures S1, S2), in line with typical behavior presented by exciplexes.^{34,41,42} Figure 2b demonstrates PL spectra in thin films of the five studied exciplex blends. The maximum steady state PL of all studied exciplexes falls within a relatively narrow range of 524–551 nm. The similarity between the exciplex emission maximum ($h\nu^{\max}$) can be rationalized with relation $h\nu^{\max} = IP_D - EA_a - E_c$, where IP_D is the ionization potential of the donors (5.5–5.7 eV), EA_a is the electron affinity of the acceptor (3.1 eV), and E_c is the electron–hole Coulombic attraction energy (also see Figure S15).^{43,44} Despite small variation in the PL spectra, the exciplex CT λ_{PL} follows the trend of the energy gap ($IP_D - EA_a$), in line with the donor strength: TCTA:TpBpTa < TAPC:TpBpTa < TPD:TpBpTa \approx TPD10:TpBpTa, except for the NPB:TpBpTa exciplex, which displays a more blue-shifted PL than expected. At this point, we note that exciplexes usually show the prompt and delayed luminescence components with slightly different PL spectra, and their contributions will be affecting the resultant steady state PL spectrum. We will return to this issue later when discussing time-resolved spectra and decay traces of exciplexes.

To understand the effects of the local triplet states (3LE) on exciplex TADF and the RISC mechanism, they have been divided into two groups: TCTA:TpBpTa and TAPC:TpBpTa, with higher triplet energy donors ($T_1 \approx 2.7$ – 2.9 eV) and TPD:TpBpTa, TPD10:TpBpTa, and NPB:TpBpTa with lower triplet energy donors ($T_1 \approx 2.4$ – 2.5 eV). This selection of donor materials allows the localization of the ${}^1CT/{}^3CT$ exciplex states significantly below the 3LE (TCTA:TpBpTa and TAPC:TpBpTa exciplexes) or slightly above it (TPD:TpBpTa, TPD10:TpBpTa, and NPB:TpBpTa exciplexes).

Note that the TpBpTa triplet energy ($T_1 = 2.75$ eV) is significantly above that of the exciplex CT in all cases.

PL decay traces for all exciplexes are presented in Figure 3. Exciplexes are complex, heterogeneous emissive systems, and

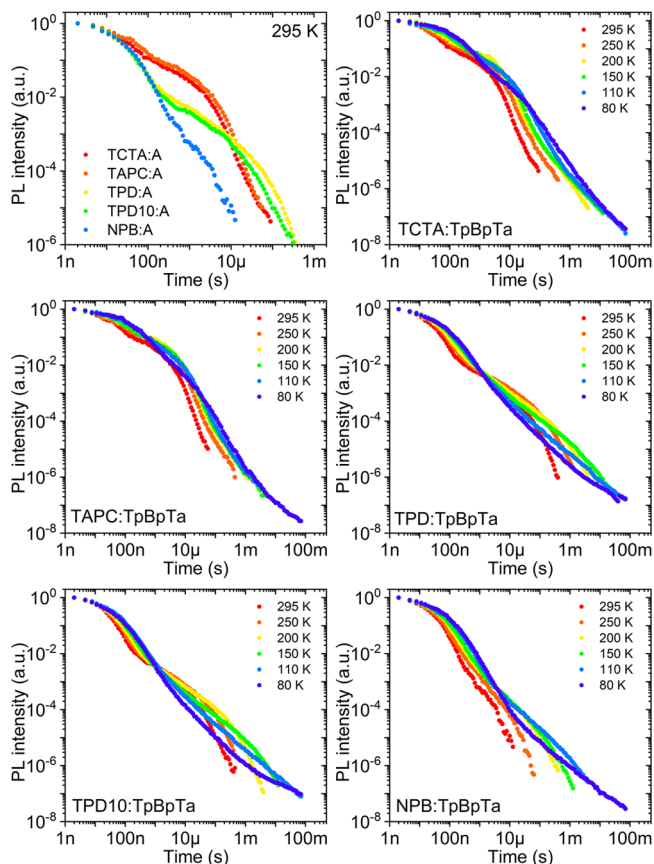


Figure 3. Photoluminescence decay in the film of all five exciplex blends as a function of temperature. The presented decay traces are obtained by integrating the photoluminescence intensity over the whole emission spectral range.

their photoluminescence decay is usually comprised of prompt and often delayed fluorescence (i.e., TADF), with both of these components being roughly monoexponential but often being better described by a bi- or multiexponential fit.^{41,45} In the exciplex systems described in this work, a monoexponential fit was used for prompt fluorescence, at delays < $1 \mu s$ (except for NPB:TpBpTa, where a biexponential fit was used), and a biexponential fit was used to fit delayed fluorescence, at delays > $1 \mu s$. We conduct laser fluence experiments on the delayed fluorescence component of each of the exciplexes, which results in a linear dependence of photoluminescence intensity with excitation dose, ruling out triplet–triplet annihilation and leaving TADF as the only possible mechanism.⁴² In this work, the RISC rates of exciplexes were estimated from average TADF lifetimes and are presented alongside other optical characteristics in Table 1.

The five exciplexes in this work can be divided into three groups based on the similarity of their photophysics behavior: TCTA:TpBpTa and TAPC:TpBpTa exciplexes (group I), TPD:TpBpTa and TPD10:TpBpTa exciplexes (group II), and the NPB:TpBpTa exciplex (group III).

The first group, the TCTA:TpBpTa and TAPC:TpBpTa exciplexes, shows the largest $\Phi_{PL} \approx 0.4$ of all investigated

Table 1. Summary of Photophysical Properties of Studied Exciplexes

exciplex	λ_{em} , nm	Φ_{PL}	τ_{PF} , ns	τ_{DF} , μs^a	$k_{PF} \times 10^{-6}$, s^{-1}	$k_{RISC} \times 10^{-6}$, s^{-1}	DF/PF
TCTA:TpBpTa	524	0.35 ± 0.04	26 ± 2	$\tau_1 = 0.40 \pm 0.06$ (61%) $\tau_2 = 2.0 \pm 0.4$ (39%) $\tau_{av} = 1.7 \pm 0.3$	2.3 ± 1.0	3.5 ± 1.4	4.8 ± 1.5
TAPC:TpBpTa	533	0.45 ± 0.14	20 ± 1	$\tau_1 = 0.26 \pm 0.04$ (59%) $\tau_2 = 1.9 \pm 0.2$ (41%) $\tau_{av} = 1.7 \pm 0.2$	2.4 ± 1.3	5.6 ± 2.1	8.3 ± 2.2
TPD:TpBpTa	551	0.07 ± 0.01	19 ± 0.6	$\tau_1 = 1.33 \pm 0.08$ (81%) $\tau_2 = 13 \pm 1$ (19%) $\tau_{av} = 9.8 \pm 1.4$	1.4 ± 0.4	~ 0.1	1.7 ± 0.3
TPD10:TpBpTa	551	0.14 ± 0.02	19 ± 0.4	$\tau_1 = 1.00 \pm 0.06$ (75%) $\tau_2 = 9.0 \pm 0.7$ (25%) $\tau_{av} = 7.0 \pm 0.8$	3.5 ± 0.6	~ 0.1	1.11 ± 0.14
NPB:TpBpTa	532	0.03 ± 0.01	$\tau_1 = 6.9 \pm 0.5$ (58%) $\tau_2 = 37 \pm 2$ (42%) $\tau_{av} = 31 \pm 3$	$\tau_1 = 0.22 \pm 0.03$ (93%) $\tau_2 = 1.8 \pm 0.4$ (7%) $\tau_{av} = 0.84 \pm 0.45$	0.8 ± 0.4	b	0.15 ± 0.08

^a τ_{av} is the average amplitude-weighted decay lifetime,^{45,47} $\tau_{av} = A_1\tau_1^2 + A_2\tau_2^2 / A_1\tau_1 + A_2\tau_2$. ^bUnable to determine with sufficient precision due to low intensity of delayed fluorescence.

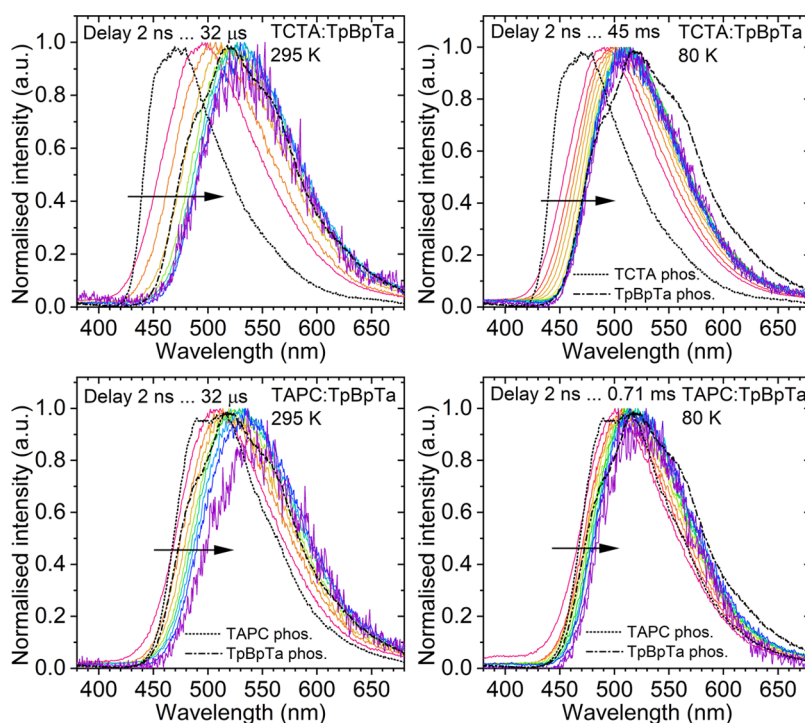


Figure 4. Time-resolved photoluminescence spectra of exciplexes TCTA:TpBpTa and TAPC:TpBpTa in film at 295 K and 80 K.

systems as well as the largest contribution of TADF, $\Phi_{DF}/\Phi_{PF} \approx 5-8$. k_{RISC} is on order of $\sim 10^6 s^{-1}$, like in other highly efficient TADF exciplexes.⁴¹ The Φ_{DF}/Φ_{PF} value of these two exciplexes is identical within the margin of error. Crucially, the steady state PL spectra of these two exciplexes are different.

In the second group, the TPD:TpBpTa and TPD10:TpBpTa exciplexes, the $\Phi_{PL} \approx 0.1$ and $\Phi_{DF}/\Phi_{PF} \approx 1-2$ are lower than in group I. The RISC rate is estimated to be at least 1 order of magnitude smaller than in TCTA:TpBpTa and TAPC:TpBpTa exciplexes. The TPD10:TpBpTa exciplex displays a visibly larger Φ_{PL} and k_{PF} but smaller Φ_{DF}/Φ_{PF} than its counterpart TPD:TpBpTa. This is a sign of a slower ISC rate and increased oscillator strength of the $S_0 \rightarrow S_1$ transition. TPD10 has a larger π system than

TPD, which results in an increased $\pi\pi^*$ character to the S_1 state—an effect somewhat similar to that reported recently in TADF emitters built on a triptycene core.⁴⁶

Finally, the NPB:TpBpTa exciplex shows the lowest $\Phi_{PL} \approx 0.03 \pm 0.01$ and clear dominance of prompt fluorescence over TADF with a very small $\Phi_{DF}/\Phi_{PF} = 0.15 \pm 0.08$ in comparison to TPD:TpBpTa and TPD10:TpBpTa exciplexes. The NPB:TpBpTa exciplex is very similar to the TPD:TpBpTa and TPD10:TpBpTa exciplexes, but the difference lays in the shorter lifetime of the triplet state of the former. The TADF component in the NPB:TpBpTa exciplex lives around an order of magnitude shorter than in the other two exciplexes, suggesting a significant influence of nonradiative decay on the T_1 state in this case. This effect can be clearly linked to the

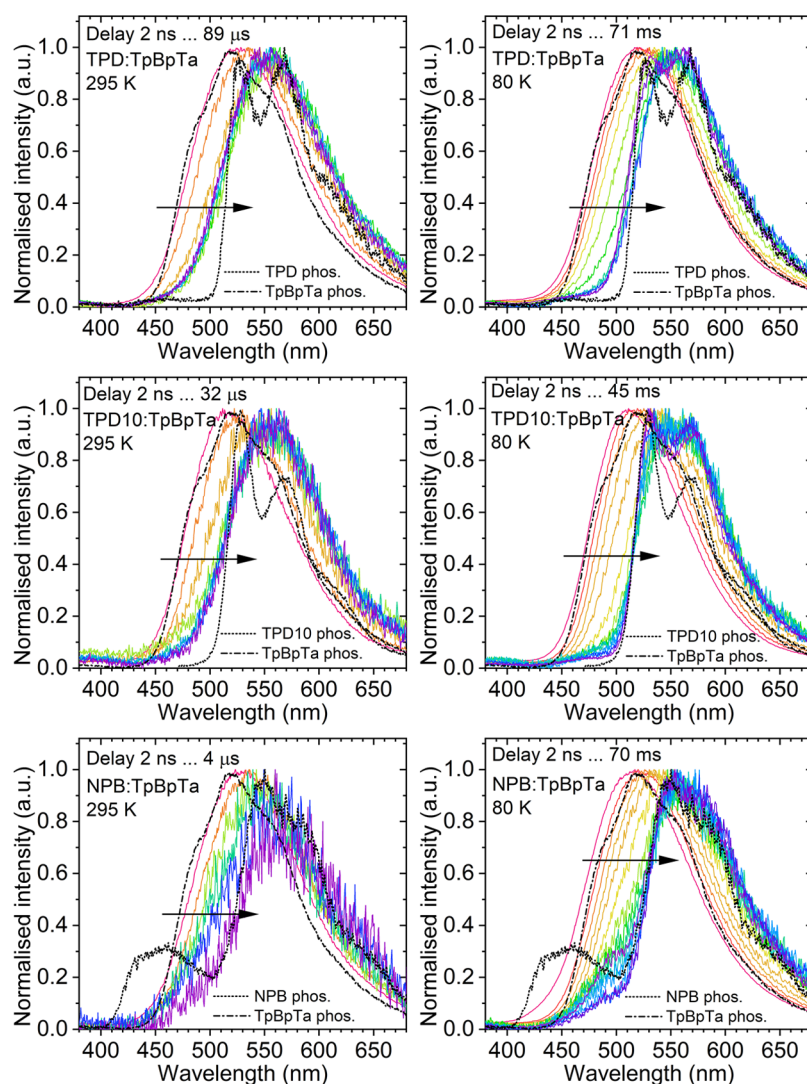


Figure 5. Time-resolved photoluminescence spectra of exciplexes TPD:TpBpTa, TPD10:TpBpTa, and NPB:TpBpTa in film at 295 K and 80 K.

local triplet state of NPB that is subject to a more intense quenching. For example, in a previously reported exciplex involving NPB, the $^1\text{CT}/^3\text{CT}$ manifold was below the ^3LE of the donor, and in this case, the differences in photophysical behavior between analogous NPB and TPD exciplexes were insignificant.⁴¹

Photoluminescence decays of all five exciplexes in the film are presented in Figure 3. The general photophysical behavior of these exciplexes is similar to that presented in related systems.⁴¹ We observe a gradual elongation of prompt and delayed fluorescence lifetimes at lower temperatures and a decrease of delayed fluorescence amplitude for TCTA:TpBpTa, TAPC:TpBpTa, TPD:TpBpTa, and TPD10:TpBpTa exciplexes, but the NPB:TpBpTa exciplex behaves differently. In the last case, we observe an increase in the long-lived component until 110 K with the first sign of intensity decrease visible at 80 K. This behavior of the NPB:TpBpTa exciplex confirms strong quenching of the NPB ^3LE state by nonradiative processes at room temperature. The behavior of all of the other exciplexes is typical of TADF emitters as the decay lifetime increases at a lower temperature—in line with the RISC mechanism.^{2,3}

Transient PL spectra recorded for the exciplex films are presented in Figures 4 and 5. We observe that the photoluminescence of exciplexes gradually redshifts with time delay. The most change occurs mainly within the first 100 ns of delay, which corresponds to prompt fluorescence. In general this behavior is attributed to geometry relaxation of the exciplex and is known among exciplexes⁴¹ and single molecule TADF emitters.⁴⁶ Prompt fluorescence originates from species that exist in an excited state for a short time without having a chance to relax their geometry, while for species emitting via delayed fluorescence there is enough time to relax their geometry or otherwise emit from a lower energy state. The states with higher energy emit at a faster rate, thus the emission spectrum redshifts due to the low energy states living longer. This behavior suggests that the CT energy of emissive states is better described as a distribution rather than a specific, discrete energy level. For this very reason, it seems more reasonable to describe CT states of the exciplex as a band which consists of a large number of CT states being close to one another in energy, although not necessarily being mixed together but rather remaining as electronic states of individual D:A pairs. Similar behavior of the transient PL spectra occurs at lower

temperatures, especially at 80 K, but the PL spectra are slightly blue-shifted with respect to those at room temperature.

Some of the exciplexes which have the ^3LE below the $^1\text{CT}/^3\text{CT}$ manifold (mostly in TPD10:TpBpTa and NPB:TpBpTa but also in TPD:TpBpTa) present phosphorescence in the long delay region beyond 1 ms, at 80 K. Phosphorescence gradually emerges in the time-resolved spectrum as delay increases due to the overlap between shorter-lived delayed fluorescence and longer-lived phosphorescence in intermediate times. Interestingly, in the NPB:TpBpTa exciplex there appears an emission shoulder to phosphorescence around 500 nm that coincides with fluorescence emission of the exciplex. This can be ascribed to the triplet–triplet annihilation (TTA) between the NPB molecules in the blend.⁴⁸ In a similar way, NPB pristine film exhibits NPB fluorescence emission in the same time delay as phosphorescence, which is again identified as TTA. Some of the exciplexes which do not display phosphorescence at lower temperatures, such as TCTA:TpBpTa and TAPC:TpBpTa, display a long-lived component at delay times exceeding 1 ms that decays in a power law fashion and is visible in the decay as a mostly linear region at the end of the decay. This decay behavior has been previously hypothesized to originate from nongeminate electron–hole recombination.^{41,49,50}

It is worth noting that, with exciplexes involving TPD, TPD10, and NPB donors, their CT energy remains always above the ^3LE energy of the donor, thus the local triplet state is the active T_1 state which mediates ISC and RISC. In this case the ^3LE state of the donor acts as a quencher of $^1\text{CT}/^3\text{CT}$ states, potentially leading to a reduction in exciplex TADF. We observe this behavior in the case of the NPB:TpBpTa blend. On the other hand, in TCTA:TpBpTa and TAPC:TpBpTa exciplexes, the bottom of the CT band remains below the energy of the lowest ^3LE , which renders these exciplexes the most efficient.

We now aim to explain the steady state spectra of exciplexes using the time-resolved data. One can observe that steady state emission of the NPB:TpBpTa exciplex is significantly blue-shifted with respect to TPD and TPD10-based exciplexes despite all three donors having near identical ionization potentials (and thus we expect them to have similar PL spectra). We note that the prompt and delayed fluorescence of these three exciplexes are virtually identical at room and low temperatures (Figure 6), therefore the divergence of the steady state spectra must be related to the different contributions of prompt fluorescence and TADF components. We note that the NPB:TpBpTa exciplex shows a significantly lower contribution

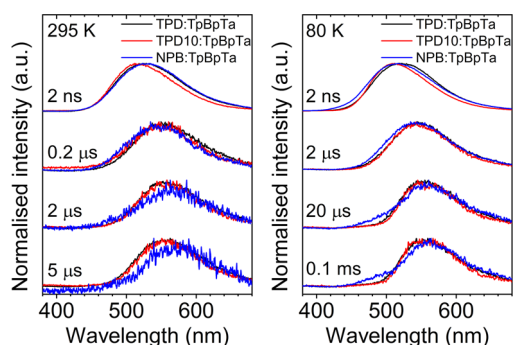


Figure 6. Overlaid time-resolved photoluminescence spectra of exciplexes TPD:TpBpTa, TPD10:TpBpTa, and NPB:TpBpTa.

of TADF than the other two exciplexes, rendering the steady-state emission prompt-dominated, which explains the blue shift in the steady state spectrum. Similarly, exciplexes with TCTA and TAPC donors display slightly different steady state spectra and prompt fluorescence at 295 K, but the TADF emission of both is identical (Figure 7). Interestingly, it appears that the

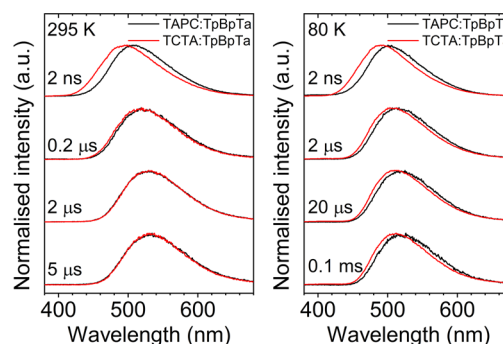


Figure 7. Overlaid time-resolved photoluminescence spectra of exciplexes TCTA:TpBpTa and TAPC:TpBpTa.

emissions differ at 80 K with the TCTA:TpBpTa emission spectra being more blue-shifted. The above-mentioned phenomena clearly demonstrate that the analysis of exciplex CT energy cannot simply rely on steady state spectra as this approach may be misleading. Instead, time-resolved spectra should be used to accurately describe exciplex CT energy.

In summary, the TCTA:TpBpTa and TAPC:TpBpTa exciplexes display the best TADF performance through a combination of factors. The ^3LE states being energetically above the $^1\text{CT}/^3\text{CT}$ manifolds provides the smallest S_1-T_1 gap, simultaneously making the ^3CT the lowest triplet excited state. While ^3LE states may often be long-lived at room temperature, they may sometimes act as a loss pathway, as observed in case of the NPB:TpBpTa exciplex. $^1\text{CT}/^3\text{CT}$ states show a much weaker coupling to the ground state, which we believe may result in a lesser susceptibility of the ^3CT state to the nonradiative decay, in line with the behavior of the said pair of exciplexes.

Theoretical Calculations. The simulated conformations of all studied exciplexes are presented in Figures S5–S9. In all cases, numerous N---HC, CH---HC, and CH--- π (T-shaped) interactions stabilize the dimers, and the corresponding binding energies are presented in Table S1. In our simulation, we assume that all of the studied complexes are even more stabilized in the solid state film, and upon the population of corresponding charge-transfer exciplex states the dimers actually do not dissociate due to the constraints by surrounding molecules; i.e., exciplexes maintain a similar close conformation to that of the ground state optimized geometry. This assumes also the small Stokes shift between vertical absorption and emission by the studied complexes, and thus S_1 and T_1 state energies calculated for S_0 optimized donor–acceptor dimers are in reasonable agreement with experimental emission wavelengths (Table S2). We used a similar approach for the simulation of charge-transfer exciplexes to that presented by Kim et al.⁵¹ with the difference that the ground state geometries of dimers were extracted from molecular dynamic simulations, while in our simulations we manually constructed initial dimers and then optimized them using a PM6 approach. Despite the PM6 approach having a known limitation for quantitatively correct estimation of

Table 2. Summary of Excited State Energies Based on Time-Resolved Photoluminescence Spectra and Theoretical CT State Energy^a

exciplex	CT energy (295 K), eV ^b	CT energy (80 K), eV ^b	CT energy (theory), eV	T ₁ (donor), eV	T ₁ (acceptor), eV	CT- ³ LE, eV ^c
TCTA:TpBpTa	2.90→2.67	2.89→2.74	3.03→2.50	2.89	2.75	-0.08
TAPC:TpBpTa	2.78→2.66	2.79→2.67	2.96→2.18	2.75		-0.09
TPD:TpBpTa	2.75→2.58	2.77→2.53 ^d	2.60→2.35	2.45		0.13
TPD10:TpBpTa	2.77→2.55	2.75→2.48 ^d	2.69→2.38	2.46		0.09
NPB:TpBpTa	2.75→2.53	2.82→2.47 ^d	2.79→2.49	2.48		0.05

^aAssume ± 0.03 eV error on all excited state energy values. ^bCT energy related to all time-resolved spectra recorded, from prompt fluorescence (≈ 2 ns delay)—larger value—to the last recorded spectra with sufficient S/N ratio—lower value. Note the CT energy is always monotonically decreasing with time delay. ^cEnergy difference between the lowest boundary of CT energy band at room temperature and the nearest ³LE level. A negative value indicates ³LE above the CT manifold. ^dVisible phosphorescence at longer delay times.

binding energies for H-bonded and Van-der-Waals complexes, the mixed-type interactions (like those in the studied exciplexes) are better described by PM6.⁵² Even if accounting for the overestimation of binding energies by the PM6 method through the systematic error contribution, the qualitative changes between different sorts of dimers are principally correct. One can see from the Table S1 that binding energies are highest for TAPC:TpBpTa dimers (in the range of 7.7–11.6 kcal mol⁻¹) and are somewhat smaller for TCTA:TpBpTa dimers (4.5–8.8 kcal mol⁻¹), while for other dimers binding energies are generally smaller (not exceeding 8.5, 6.9, and 7.4 kcal mol⁻¹ for NPB:TpBpTa, TPD:TpBpTa, and TPD10:TpBpTa dimers). This means that the propeller-shaped structure of TCTA and half-propeller-shaped structure of TAPC donor molecules are preferable for complexing with the star-shaped TpBpTa acceptor. This correlates with higher Φ_{PL} values for TAPC:TpBpTa and TCTA:TpBpTa exciplexes compared to other systems (Table 1). Blue shifted prompt fluorescence of exciplexes can be explained in terms of stronger exchange interactions between close-lying donor and acceptor counterparts that increase the transition dipole moment of the S₁(CT)–S₀ transition and shift this transition to higher energy. Indeed, one can note from the time-resolved photoluminescence spectra (Figures 4 and 5) that fast emission (in the nanosecond time scale) takes place at higher energies and with higher intensities, which corresponds to prompt fluorescence by strongly coupled exciplexes. Less coupled exciplexes generally demonstrate red-shifted emission and smaller intensities of S₁(CT)–S₀ transition that results in a decrease of prompt fluorescence intensity and facilitates the TADF channel with higher fluorescence lifetimes. This means the key role of geometrical configuration and exchange interactions in the photophysical behavior of exciplexes. One can see from Table 2 that our theoretical estimations for just 10 random exciplex configurations reproduce (both qualitatively and quantitatively) the experimental trends in ¹CT energy well, confirming the presented hypothesis about the correlation between the coupling strength within dimer pairs and emission energy/intensity/lifetime.

In order to bring more insight into the electronic transitions governing RISC and ISC and thus the TADF mechanism, we analyze the orbital topology of higher-lying triplet excited states of all exciplexes at orientation 1. The orbital contours relevant to this discussion are presented in Supporting Figures S3.6–S3.10. For NPB:TpBpTa exciplex, the T₂ state is of mixed ³CT+³LE nature localized on a donor NPB state. The existence of this state is favorable for T₁–S₁ RISC, as vibronic coupling between T₂ and T₁ (intermolecular CT) should be efficient through the small energy gap and different spatial

symmetry reasons. However, the radiative decay of this exciplex is hindered by the nonradiative processes, as discussed earlier. In the TAPC:TpBpTa exciplex, the ³LE state of TAPC counterpart is lying much higher in energy than the T₁ intermolecular ³CT state. One should note that T₂–T₄ states for the TAPC:TpBpTa in conformation 1 are all of an intermolecular ³CT nature, while T₅ at 2.95 eV mainly corresponds to a state localized on the TpBpTa acceptor. The position of the ³LE state of TAPC is thus higher by 0.75 eV relative to the T₁ (³CT) state of the TAPC:TpBpTa exciplex. The situation is very similar for the TCTA:TpBpTa exciplex: the T₂ state corresponds to the intermolecular ³CT state, while the ³LE state of the TpBpTa acceptor is predicted to remain 0.4 eV higher than the T₁ intermolecular ³CT state, while the ³LE state of TCTA is 0.5 eV higher than the T₁. For TPD:TpBpTa and TPD10:TpBpTa exciplexes, the T₂ state is of a similar intermolecular CT nature to the T₁ state, while the ³LE states (both for donor and acceptor) are predicted near 2.9 eV, corresponding to higher-lying triplet T_n states ($n > 4$). From this picture, we can conclude that exciplexes with lower energy ³LE, such as NPB:TpBpTa, display RISC/ISC mediated through the said local triplet state as its orbital topology is significantly different from that of the S₁/T₁ CT states. However, the exciplexes with high-lying ³LE do not rely on these states for the RISC/ISC mechanism. Instead, the upper (i.e., $n = 2$) T_n intermolecular CT state serves as the mediator state with its topology being different from that of the S₁/T₁ CT states. This demonstrates that ³LE states are not necessary for efficient TADF and in fact close-lying intermolecular CT states spin–orbit couple sufficiently strongly to allow fast spin flip.

OLED Fabrication and Characterization. In order to evaluate the TADF behavior of studied exciplex systems under electrical excitation, we have introduced them as emitters in thermally evaporated multilayer OLEDs. The structures of the fabricated prototype devices were as follows: ITO/NPB (40 nm)/TCTA (10 nm)/TCTA:TpBpTa (20 nm)/TpBpTa (50 nm)/LiF (1 nm)/Al (100 nm); ITO/NPB (30 nm)/TAPC (10 nm)/TAPC:TpBpTa (20 nm)/TpBpTa (50 nm)/LiF (1 nm)/Al (100 nm); ITO/NPB (30 nm)/TPD (10 nm)/TPD:TpBpTa (20 nm)/TpBpTa (50 nm)/LiF (1 nm)/Al (100 nm); ITO/TAPC (20 nm)/TPD10 (10 nm)/TPD10:TpBpTa (20 nm)/TpBpTa (50 nm)/LiF (1 nm)/Al (100 nm); ITO/TAPC (30 nm)/NPB (10 nm)/NPB:TpBpTa (20 nm)/TpBpTa (50 nm)/LiF (1 nm)/Al (100 nm).

The emitting layer of OLEDs comprised codeposited donor and acceptor materials at a 1:1 ratio. The schematic representation of the energy levels of organic semiconductors used in the OLEDs is shown in Figure S15.

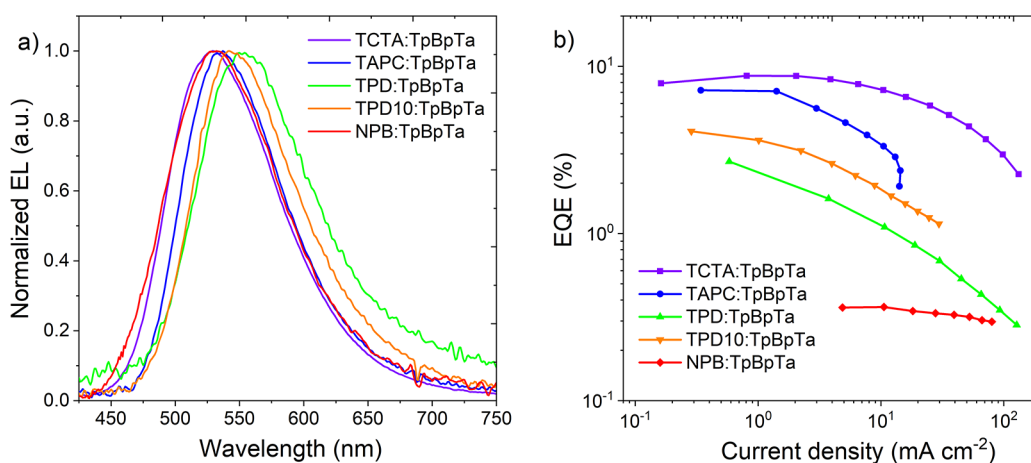


Figure 8. Electroluminescence (EL) spectra of fabricated devices (a) and their external quantum efficiency versus current density characteristics (b).

Table 3. Characteristics of OLED Devices: Turn-on Voltage (V_{on}), Maximum Brightness (L_{max}), Current Efficiency ($\eta_{L,\text{max}}$), External Quantum Efficiency ($\eta_{\text{ext,max}}$), Maxima of PL and EL (λ_{max}) Spectra, CIE 1931 Color Coordinates, Current Efficiency (η_L), Power Efficiency (η_p), and External Quantum Efficiency (η_{ext}) at 100 cd m^{-2} and 1000 cd m^{-2} Brightness

	V_{on} (V)	L_{max} (cd m^{-2})	$\eta_{L,\text{max}}$ (cd A^{-1})	$\eta_{\text{ext,max}}$ (%)	λ_{max} PL (nm)	λ_{max} EL (nm)	CIE 1931 (x; y)	100 cd m^{-2}		1000 cd m^{-2}	
								η_L (cd A^{-1})	η_{ext} (%)	η_L (cd A^{-1})	η_{ext} (%)
TCTA:TpBpTa	2.5	9340	29.4	8.8	525	529	(0.34; 0.56)	26.9	8.4	27.1	8.3
TAPC: TpBpTa	2.5	1230	25.6	7.2	537	536	(0.36; 5.58)	24.7	7.2	13.1	3.8
TPD: TpBpTa	2.5	1095	8.2	2.7	549	552	(0.41; 0.56)	6.6	2.0	1.1	0.4
TPD10: TpBpTa	2.5	1061	12.2	4.1	548	544	(0.40; 0.56)	12.2	3.7	3.8	1.2
NPB: TpBpTa	2.5	703	1.1	0.37	537	533	(0.32; 0.50)	1.1	0.36		

The main electroluminescence properties of the OLEDs are presented in Figures 8 and S16, and Table 3. All devices exhibit pure green electroluminescence in line with the PL spectra of the respective exciplexes (Figure S17), with λ_{EL} in the range of 530–555 nm. The EL spectra are not contaminated by emission from adjacent layers and remain stable with increasing operating voltage. It should be noted that all fabricated OLEDs exhibit a relatively low turn on voltage of 2.5 V. The above facts show the OLEDs have a barrier-free structure and efficient hole and electron transport resulting in an effective exciton recombination in the active layer.

Additionally, the presented devices were designed in order to display a similar current density operating regime which facilitates comparison of electroluminescence properties between exciplexes. The current density–voltage curves of OLEDs are presented in Figure S16. All of them are similar except for the TCTA:TpBpTa blend, which displays a characteristic slightly shifted to higher voltages. Such a shift is caused by a deeper HOMO energy (5.7 eV) of TCTA molecules than other electron-donating materials used in the study, resulting in a slightly larger barrier for hole transport.

TCTA:TpBpTa and TAPC:TpBpTa exciplexes give higher OLED efficiency than the other three. Among these two, TCTA:TpBpTa presents the best device performance with the maximum brightness (L_{max}), maximum current efficiency ($\eta_{L,\text{max}}$), and maximum external quantum efficiency ($\eta_{\text{ext,max}}$) being 9340 cd m^{-2} , 29.4 cd A^{-1} , and 8.8%, respectively. The device fabricated with the TAPC:TpBpTa exciplex exhibits a comparable performance with an L_{max} of 1230 cd m^{-2} , $\eta_{L,\text{max}}$ of 25.6 cd A^{-1} , and $\eta_{\text{ext,max}}$ of 7.2%, respectively. The second group of devices made using TPD:TpBpTa and

TPD10:TpBpTa exciplexes in the emissive layer exhibits a 2–3-fold lower performance than the most efficient OLEDs in this work. The maximum brightness (L_{max}), current efficiency ($\eta_{L,\text{max}}$), and external quantum efficiency ($\eta_{\text{ext,max}}$) obtained are 1095 cd m^{-2} , 8.2 cd A^{-1} , and 2.7% for a device employing the TPD:TpBpTa exciplex, respectively, and 1061 cd m^{-2} , 12.2 cd A^{-1} , and 4.7% for OLED based on the TPD10:TpBpTa blend, respectively. Despite the similarity of these two exciplex systems, TPD10:TpBpTa gives better performance than TPD:TpBpTa. This can be rationalized by a higher photoluminescence quantum yield in the former. Finally, the NPB:TpBpTa exciplex displays the lowest OLED performance due to a strong quenching of triplet states. We record an $\eta_{\text{ext,max}}$ of 0.37% and an $\eta_{L,\text{max}}$ of 1.1 cd A^{-1} for OLED using this exciplex in the emissive layer. The maximum external quantum efficiency of OLED devices agrees with the Φ_{PL} of respective exciplexes in film.

Charge Trapping Properties of Exciplex Emitters. It is known that charge trapping may affect, directly or indirectly, processes of photogeneration and recombination of charge carriers, so it may have a strong influence on the performance of OLEDs. In electroluminescent devices, the charge transport depends not only on the electronic properties of semiconducting molecules, but also on the supramolecular structure of the active layer, which determines the density of transport states and trapping sites. The presence of trap states hinders the transport process of carriers in the OLED and affects the shape of the current–voltage characteristics and also the luminance–current density dependence of OLEDs. For that reason, the trapping and recombination processes in investigated exciplex blends were examined by spectrally

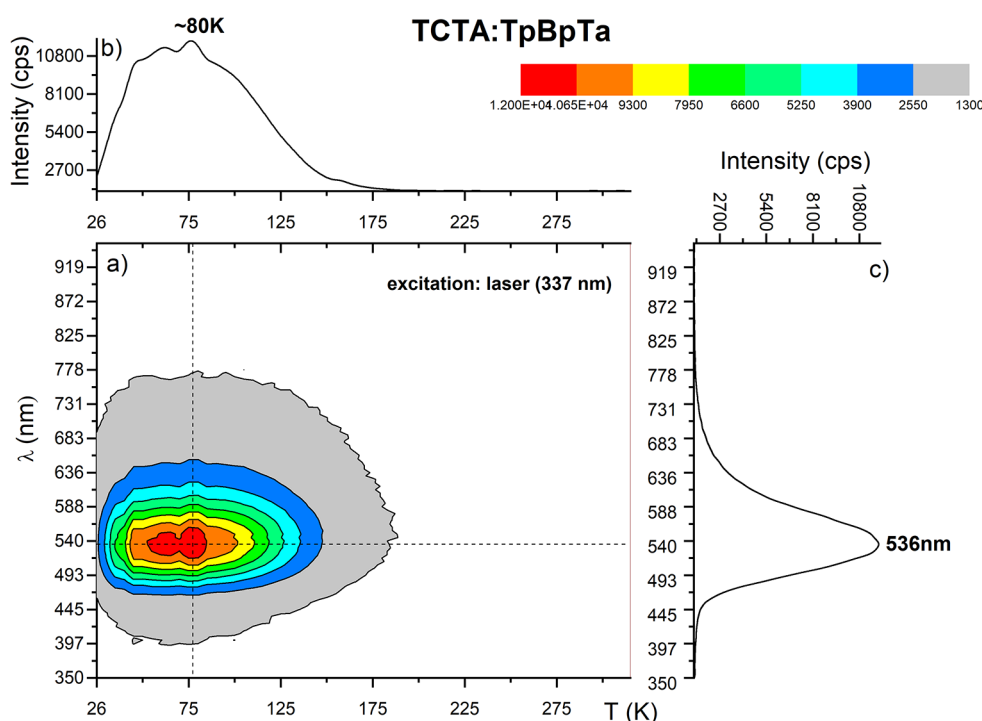


Figure 9. SRTL spectra of the TCTA:TpBpTa film. (a) SLTL map. (b) Normalized monochromatic TL curve recorded at emission maximum ($\lambda = 536$ nm). (c) Isothermal spectrum of emitted light recorded at the temperature corresponding to TL maximum. Straight dashed lines on the SRTL map indicate the selected wavelength for the monochromatic TL curve (horizontal line) and the selected temperature for the isothermal spectrum of emitted light (vertical line).

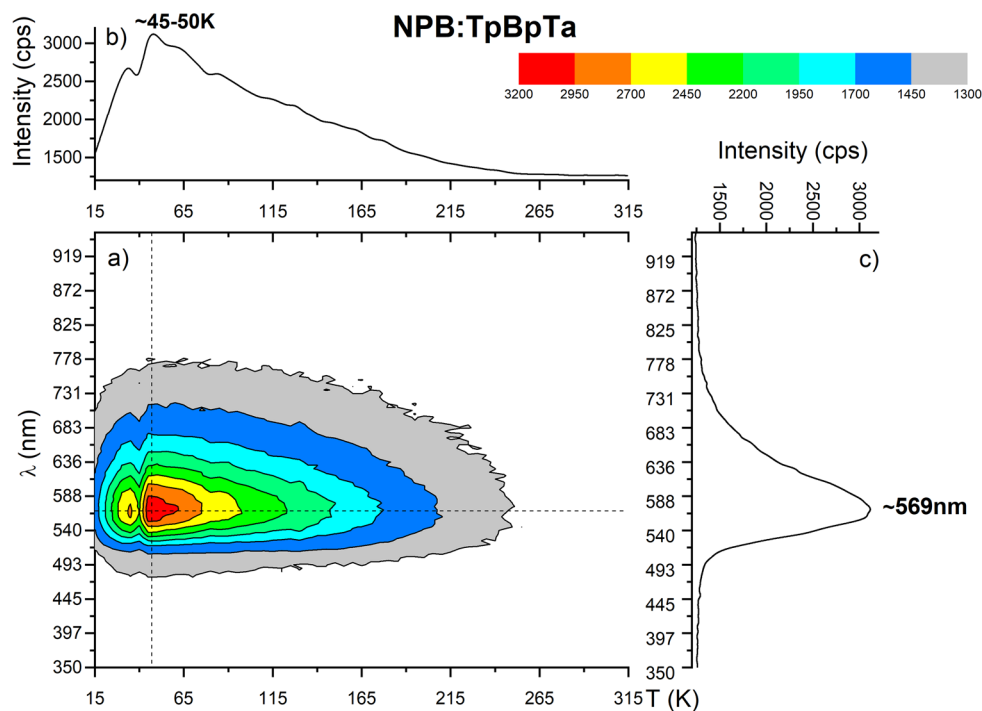


Figure 10. SRTL spectra of the NPB:TpBpTa film. (a) SRTL map. (b) Normalized monochromatic TL curve recorded at emission maximum ($\lambda = 569$ nm). (c) Isothermal spectrum of emitted light recorded at the temperature corresponding to TL maxima. Straight dashed lines on the SRTL map indicate the selected wavelength for the monochromatic TL curve (horizontal line) and the selected temperature for the isothermal spectrum of emitted light (vertical line).

resolved thermoluminescence (SRTL). This is one of the direct methods for studying the phenomenon of trapping charge carriers in electroluminescent organic materials.⁵³ The TL experiment involves excitation of the sample at a

wavelength corresponding to the lowest energy absorption band at the lowest temperature available in a given setup. Optical excitation generates singlet excitons, which can either recombine radiatively or nonradiatively, or dissociate. Most of

the photogenerated carriers recombine quickly, but some of them avoid geminate recombination. After the thermalization process, these charge carriers remain in localized states at some separation distance. When the sample is warming up, the trapped charge carriers are being released from traps, at first from the most shallow traps and then from gradually deeper ones. If the released charges recombine with an oppositely charged counterpart, a thermoluminescence signal can be observed. Occupation and depth of trap states can be inferred from intensity and position of the TL trace maxima. The process leading to light generation in TL is similar to electroluminescence. When the injected holes and electrons migrate through the device, persistently bound polaron pairs are formed once the electrostatic attraction between them exceeds thermal energy. In this limit, charge carriers recombine following degenerate spin statistics (a singlet/triplet ratio of 1:3).

SRTL maps for studied exciplex blends are presented in Figures 9, 10, and S18–S20. For all of the films except NPB:TpBpTa (Figure 10), a broad thermoluminescence (TL) band (detection at $\lambda = 536$ nm) with a maximum at *ca.* 80 K is observed (Figures S18–S20). Broad and blurred maxima in TL spectra are characteristic of disordered materials and are connected with the broad distribution of the trap states' energy. The comparison of isothermal spectra of emitted light recorded at temperatures corresponding to SRTL maxima (Figures 9c and S18–S20) with time-resolved photoluminescence spectra suggests that the radiative recombination centers are localized on exciplex CT states. Interestingly, a different shape of the monochromatic TL spectrum was obtained for the NPB:TpBpTa exciplex (Figure 10). The maximum of this TL band is shifted to a lower temperature (~ 45 K) in comparison with other exciplexes, pointing at the dominant role of shallower traps in this system.

The analysis of energy of states of exciplexes in films (local donor and acceptor singlet and triplet states and intermolecular CT states) combined with the SRTL results allows concluding that the traps are connected mainly with the CT states of exciplexes. However, in the case of NPB:TpBpTa, the comparison of the isothermal spectrum measured at the TL maximum with the photoluminescence spectra recorded at 80 K after a 70 ms delay time and the phosphorescence spectrum of pure NPB leads to the conclusion that, for this system, ^3LE states are involved in radiative recombination processes in thermoluminescence. The difference between the depth of traps observed in TL spectra of NPB:TpBpTa and TCTA:TpBpTa can be explained when we consider the broad energy distribution of the $^1\text{CT}/^3\text{CT}$ exciplex states and the localization of the ^3LE , discussed earlier in the text. We can assume that in both cases the traps are localized on the lowest triplet CT states (at the bottom of the CT band) and upon heating, the trapped charge carriers are released, but in TCTA:TpBpTa the depth of traps is defined by the width of the CT energy band, whereas in NPB:TpBpTa the charge carriers are moved to ^3LE of the donor where they recombine radiatively. The energy difference between the lowest boundary of CT energy band and the nearest ^3LE level for investigated systems (Table 2) seems to support this interpretation. It is worth noting that all TL spectra are broad and for almost all exciplexes a long tail even up to 220 K can be observed. However, the shape and the maximum position of isothermal spectra stay unchanged when the temperature increases. This indicates a broad distribution of

trap energy, which can arise from differences in the local molecular conformation and the geometry of created exciplexes.

A comparison between the PL, EL, and the SRTL spectra in the NPB:TpBpTa exciplex (Figure S21) shows a variety of recombination states, which take part in radiative recombination processes. Deactivation of donor triplets results in TL spectra resembling NPB phosphorescence, while in EL and PL the intermolecular CT emission dominates. In the TCTA:TpBpTa (Figure S21) exciplex, CT states play a dominant role in the radiative recombination in all cases.

CONCLUSIONS

We have studied five exciplexes with similar intermolecular CT energies, and we rationalize their divergent behavior with the relative energy of the said CT state and the ^3LE state of the donor. Generally speaking, the ^3LE state may introduce additional triplet quenching channels and is most desired to remain above the CT manifold. At the same time, the ^3LE state is irrelevant for the RISC mechanism as usually there exists sufficient density of upper CT states with different orbital geometries for the S_1/T_1 CT. In this way, ^3LE is not necessary for efficient RISC as it can be mediated by the said upper CT states.^{54,55}

We were able to rationalize the commonly observed temporal red shift in time-resolved spectra of exciplexes. Stronger coupled exciplexes display higher energy (blue-shifted) CT and a larger $\text{S}_1 \rightarrow \text{S}_0$ decay rate, contributing more to prompt fluorescence. Weakly coupled exciplexes show lower energy (red-shifted) CT and a lower $\text{S}_1 \rightarrow \text{S}_0$ decay rate, leading to a larger contribution of ISC, thus contributing more to the TADF component.

Furthermore, we have investigated trapping/detrapping phenomena and radiative recombination processes in exciplex layers by spectrally resolved thermoluminescence (SRTL). The experiment provides an assumption that the radiative recombination centers as well as shallow traps are mainly distributed on exciplex intermolecular CT states.

Finally, we have demonstrated the use of the studied exciplex blends in proof-of-concept OLEDs. The performance of OLED devices closely follows their photophysical behavior with the best result obtained for the TCTA:TpBpTa and TAPC:TpBpTa blends showing maximum external quantum efficiencies (EQE) of 8.8% and 7.2%, respectively. The favorable charge transporting/trapping properties prove the unique characteristics of exciplexes as exceptional emitters or hosts in OLEDs.

EXPERIMENTAL SECTION

Photophysics. UV–vis absorption spectra of thin films were recorded on a Cary 5000 (Varian) spectrometer. Steady-state photoluminescence spectra of samples were performed at room temperature with an Edinburgh Instruments FLS980 fluorescence spectrometer (Edinburgh Instruments Ltd., Livingston, UK) with a Xe lamp as an excitation source and an R-928 photomultiplier detector. Time-resolved photoluminescence and PL decays were realized using nanosecond gated luminescence and lifetime measurements (from 400 ps to 1 s) using either third harmonics of a high energy pulsed Nd:YAG laser emitting at 355 nm (EKSPLA) or a N_2 laser emitting at 337 nm. PF/DF time-resolved measurements were performed by exponentially increasing gate and integration times.⁵⁶ Temperature-dependent experiments were conducted using a nitrogen cryostat (Janis Research). The photoluminescence quantum yields (PLQY) of thin films in a nitrogen atmosphere were measured

using a QePro spectrometer (Ocean Optics) coupled with an integrating sphere (Labsphere) and LED light source (Ocean Optics) using a method described elsewhere.⁵⁷ All films for photophysical studies were deposited from chloroform solutions by drop-cast or spin-coat with a 1:1 weight ratio of donor and acceptor.

Thick layers (thickness in a 2–3 μm range) of exciplex blends for spectrally resolved thermoluminescence (SRTL) experiments were obtained by drop-casting from chloroform solutions onto aluminum substrates. Then, samples were placed between a thermostatic holder and sapphire glass in a vacuum chamber (closed-cycle cryogenic system APD Cryogenics). The SRTL experiment was conducted for all exciplex blends in the 15–325 K temperature range under a heating rate of 7 K min^{-1} after photoexcitation at 15 K by a pulsed nitrogen laser ($\lambda = 337 \text{ nm}$; PTL, model GL-3300). Thermoluminescence was recorded by a detection system consisting of an optical collector, optical-fiber cable, a Micro HR Imaging Spectrograph, and a CCD camera (Horriba Jobin-Yvon). The detailed SRTL experimental procedure was described previously.^{58,59}

Theoretical Calculations. Initial configurations of donor–acceptor molecular pairs (donor molecules are NPB, TAPC, TCTA, TPD, and TPD10, while the acceptor molecule is TpBpTa) were constructed by the manual approach of molecules by different interacting sites with intermolecular distances of 3–3.5 Å. For each donor–acceptor combination, 10 different pair configurations were constructed and then optimized in ground singlet state (S_0) by the PM6 semiempirical method,⁶⁰ which works well for predicting the structure of intermolecular complexes with mixed types of interactions and requires small computational costs. For each optimized dimer, the energies of S_1 and T_1 vertical excited states were calculated using a time-dependent (TD) density functional theory (DFT) method by using a ωB97XD range-separated functional⁶¹ ($\omega = 0.05$) and 6-31G(d) basis set.^{62,63} This approach is somewhat similar to those used by Kim et al.⁵¹ who used molecular dynamic simulations for predicting initial configurations of donor–acceptor molecular pairs and then utilized the similar $\omega\text{B97X}/6\text{-}31\text{+G(d,p)}$ method (without dispersion correction)^{61–64} with $\omega = 0.05$ and the PBF solvation model for predicting S_1 and T_1 energies of exciplexes. In our calculations, we did not use a solvent model and calculated S_1 and T_1 state energies in a gas phase approximation that corresponds to the experimental conditions of thin solid film photophysical measurements. All of the calculations were performed using Gaussain 16 software (revision A.03).⁶⁵

Devices. Electroluminescent devices have been fabricated on precleaned, patterned indium–tin–oxide (ITO)-coated glass substrates with a sheet resistance of 20 Ω/sq and an ITO thickness of 100 nm (Ossila Ltd., Sheffield, UK). Organic semiconductors have been purchased from commercial sources (Lumtec, Sigma-Aldrich) and were purified by temperature-gradient sublimation in a vacuum. All materials and the cathode layer were thermally deposited in a Kurt J. Lesker Spectros II evaporation system under a pressure of 10^{-6} mbar without breaking the vacuum. The sizes of active pixels were 8 mm^2 and 16 mm^2 . NPB (N,N' -di(1-naphthyl)- N,N' -diphenyl-(1,1'-biphenyl)-4,4'-diamine) or TAPC (4,4'-cyclohexylidenebis[N,N -bis(4-methylphenyl)benzenamine]) were used as a hole injection layer (HIL). TCTA (tris(4-carbazoyl-9-ylphenyl)amine), TAPC, TPD (N,N' -bis(3-methylphenyl)- N,N' -diphenylbenzidine), TPD10 (N_4,N_4' -di(biphenyl-4-yl)- N_4,N_4' -diphenylbiphenyl-4,4'-diamine) and NPB were introduced as a hole transport layer (HTL) depending on the architecture of the devices. TpBpTa:2,4,6-tris(3'-(pyridin-3-yl)biphenyl-3-yl)-1,3,5-triazine was adopted as a hole blocking layer (HBL) and electron transport layer (ETL). Lithium fluoride (LiF) and aluminum were used as the cathode. Organic semiconductors and aluminum were deposited at a rate of 1 Å s^{-1} , and the LiF layer was deposited at 0.1 Å s^{-1} . Thicknesses and evaporation rates of deposited materials were monitored with a crystal microbalance. In the case of electron donating (D) materials for the exciplex, the following have been used: TCTA, TAPC, TPD, TPD10, NPB, and electron-accepting TpBpTa. The active layer was achieved by coevaporating donor and acceptor materials at the same time with identical rates. The characteristics of the devices were recorded using a 10 inch

integrating sphere (Labsphere) connected to a source meter unit and Ocean Optics USB4000 spectrometer in a glovebox.⁶⁶

■ ASSOCIATED CONTENT

Supporting Information

The Supporting Information is available free of charge at <https://pubs.acs.org/doi/10.1021/acsaelm.2c01518>.

Absorption and photoluminescence (PL) spectra of the donors (D) and acceptor (A) and of their blends, time-resolved PL spectra, excitation power dependence of delayed fluorescence, molecular orbital contours and details of theoretical calculations, energy level diagrams of OLED structures, device performance, and supplementary thermoluminescence (TL) spectra (PDF)

■ AUTHOR INFORMATION

Corresponding Authors

Piotr Pander – Faculty of Chemistry, Silesian University of Technology, 44-100 Gliwice, Poland; Centre for Organic and Nanohybrid Electronics, Silesian University of Technology, 44-100 Gliwice, Poland; Department of Physics, Durham University, Durham DH1 3LE, United Kingdom; Email: piotr.pander@polsl.pl

Glib V. Baryshnikov – Department of Chemistry and Nanomaterials Science, Bohdan Khmelnytsky National University, 18031 Cherkasy, Ukraine; Laboratory of Organic Electronics, Department of Science and Technology, Linköping University, SE-60174 Norrköping, Sweden; orcid.org/0000-0002-0716-3385; Email: glib.baryshnikov@liu.se

Authors

Marian Chapran – Department of Molecular Physics, Lodz University of Technology, 90-924 Lodz, Poland; Present Address: MICROOLED S.A.S., 7 parvis Louis Neel, 38000 Grenoble, France; orcid.org/0000-0002-2411-9642

Ihor Sahalianov – Bioelectronics Materials and Devices Laboratory, Central European Institute of Technology CEITEC, Brno University of Technology, 61200 Brno, Czech Republic

Nataliya N. Karaush-Karmazin – Department of Chemistry and Nanomaterials Science, Bohdan Khmelnytsky National University, 18031 Cherkasy, Ukraine

Gabriela Wiosna-Salyga – Department of Molecular Physics, Lodz University of Technology, 90-924 Lodz, Poland; orcid.org/0000-0002-4658-7922

Ireneusz Glowacki – Department of Molecular Physics, Lodz University of Technology, 90-924 Lodz, Poland

Beata Luszczynska – Department of Molecular Physics, Lodz University of Technology, 90-924 Lodz, Poland

Complete contact information is available at: <https://pubs.acs.org/doi/10.1021/acsaelm.2c01518>

Notes

The authors declare no competing financial interest.

■ ACKNOWLEDGMENTS

M.C. is grateful for support from the National Science Center in Poland, Project No. 2018/31/N/ST4/03459. G.B. thanks, for support, the Swedish Research Council (Starting Grant No. 2020-04600). N.K.-K. and G.B. thank the Ministry of

Education and Science of Ukraine for support (Project No. 0121U107533). The quantum-chemical calculations were performed with computational resources provided by Swedish National Infrastructure for Computing (SNIC 2022/5-103) at the High-Performance Computing Center North (HPC2N) partially funded by the Swedish Research Council through the Grant Agreement No. 2018-05973. P.P. thanks Prof. Fernando B. Dias and Prof. Andy P. Monkman for providing access to research equipment.

REFERENCES

- (1) Baldo, M. A.; O'Brien, D. F.; Thompson, M. E.; Forrest, S. R. Excitonic Singlet-Triplet Ratio in a Semiconducting Organic Thin Film. *Phys. Rev. B* **1999**, *60* (20), 14422–14428.
- (2) Yersin, H.; Rausch, A. F.; Czerwieniec, R.; Hofbeck, T.; Fischer, T. The Triplet State of Organo-Transition Metal Compounds. Triplet Harvesting and Singlet Harvesting for Efficient OLEDs. *Coord. Chem. Rev.* **2011**, *255*, 2622–2652.
- (3) Uoyama, H.; Goushi, K.; Shizu, K.; Nomura, H.; Adachi, C. Highly Efficient Organic Light-Emitting Diodes from Delayed Fluorescence. *Nature* **2012**, *492* (7428), 234–238.
- (4) Dias, F. B. Kinetics of Thermal-Assisted Delayed Fluorescence in Blue Organic Emitters with Large Singlet–Triplet Energy Gap. *Philos. Trans. R. Soc. A Math. Phys. Eng. Sci.* **2015**, *373*, 20140447.
- (5) Wong, M. Y.; Zysman-Colman, E. Purely Organic Thermally Activated Delayed Fluorescence Materials for Organic Light-Emitting Diodes. *Adv. Mater.* **2017**, *29* (22), 1605444.
- (6) Xiang, Y.; Gong, S.; Zhao, Y.; Yin, X.; Luo, J.; Wu, K.; Lu, Z.-H.; Yang, C. Asymmetric-Triazine-Cored Triads as Thermally Activated Delayed Fluorescence Emitters for High-Efficiency Yellow OLEDs with Slow Efficiency Roll-Off. *J. Mater. Chem. C* **2016**, *4* (4), 9998–10004.
- (7) Goushi, K.; Yoshida, K.; Sato, K.; Adachi, C. Organic Light-Emitting Diodes Employing Efficient Reverse Intersystem Crossing for Triplet-to-Singlet State Conversion. *Nat. Photonics* **2012**, *6* (4), 253–258.
- (8) Foster, R. *Organic Charge-Transfer Complexes*; Academic Press: London, 1969.
- (9) Singh, S. P.; Mohapatra, Y. N.; Qureshi, M.; Sundar Manoharan, S. White Organic Light-Emitting Diodes Based on Spectral Broadening in Electroluminescence Due to Formation of Interfacial Exciplexes. *Appl. Phys. Lett.* **2005**, *86* (11), 113505.
- (10) Goushi, K.; Adachi, C. Efficient Organic Light-Emitting Diodes through up-Conversion from Triplet to Singlet Excited States of Exciplexes. *Appl. Phys. Lett.* **2012**, *101* (2), No. 023306.
- (11) Ullbrich, S.; Benduhn, J.; Jia, X.; Nikolis, V. C.; Tvingstedt, K.; Piersimoni, F.; Roland, S.; Liu, Y.; Wu, J.; Fischer, A.; Neher, D.; Reineke, S.; Spoltore, D.; Vandewal, K. Emissive and Charge-Generating Donor–Acceptor Interfaces for Organic Optoelectronics with Low Voltage Losses. *Nat. Mater.* **2019**, *18* (5), 459–464.
- (12) Pang, Z.; Sun, D.; Zhang, C.; Baniya, S.; Kwon, O.; Vardeny, Z. V. Manipulation of Emission Colors Based on Intrinsic and Extrinsic Magneto-Electroluminescence from Exciplex Organic Light-Emitting Diodes. *ACS Photonics* **2017**, *4* (8), 1899–1905.
- (13) Song, L.; Hu, Y.; Liu, Z.; Lv, Y.; Guo, X.; Liu, X. Harvesting Triplet Excitons with Exciplex Thermally Activated Delayed Fluorescence Emitters toward High Performance Heterostructured Organic Light-Emitting Field Effect Transistors. *ACS Appl. Mater. Interfaces* **2017**, *9* (3), 2711–2719.
- (14) Cherpak, V.; Gassmann, A.; Stakhira, P.; Volyniuk, D.; Grazulevicius, J. V.; Michaleviciute, A.; Tomkeviciene, A.; Barylo, G.; von Seggern, H. Three-Terminal Light-Emitting Device with Adjustable Emission Color. *Org. Electron.* **2014**, *15* (7), 1396–1400.
- (15) Bai, R.; Meng, X.; Wang, X.; He, L. Color-Stable, Efficient, and Bright Blue Light-Emitting Electrochemical Cell Using Ionic Exciplex Host. *Adv. Funct. Mater.* **2021**, *31* (3), 2007167.
- (16) Lundberg, P.; Tsuchiya, Y.; Lindh, E. M.; Tang, S.; Adachi, C.; Edman, L. Thermally Activated Delayed Fluorescence with 7% External Quantum Efficiency from a Light-Emitting Electrochemical Cell. *Nat. Commun.* **2019**, *10* (1), 5307.
- (17) Zhao, J.; Zheng, C.; Zhou, Y.; Li, C.; Ye, J.; Du, X.; Li, W.; He, Z.; Zhang, M.; Lin, H.; Tao, S.; Zhang, X. Novel Small-Molecule Electron Donor for Solution-Processed Ternary Exciplex with 24% External Quantum Efficiency in Organic Light-Emitting Diode. *Mater. Horizons* **2019**, *6* (7), 1425–1432.
- (18) Hu, Y.; Yu, Y.; Yuan, Y.; Jiang, Z.; Liao, L. Exciplex-Based Organic Light-Emitting Diodes with Near-Infrared Emission. *Adv. Opt. Mater.* **2020**, *8* (7), 1901917.
- (19) Zheng, C.; Zhang, X. Thermally Activated Delayed Fluorescence Exciplexes in Organic Light-Emitting Diodes. In *Thermally Activated Delayed Fluorescence Organic Light-Emitting Diodes (TADF-OLEDs)*; Elsevier, 2022; pp 353–426.
- (20) Hong, G.; Gan, X.; Leonhardt, C.; Zhang, Z.; Seibert, J.; Busch, J. M.; Bräse, S. A Brief History of OLEDs—Emitter Development and Industry Milestones. *Adv. Mater.* **2021**, *33* (9), 2005630.
- (21) Jankus, V.; Data, P.; Graves, D.; McGuinness, C.; Santos, J.; Bryce, M. R.; Dias, F. B.; Monkman, A. P. Highly Efficient TADF OLEDs: How the Emitter-Host Interaction Controls Both the Excited State Species and Electrical Properties of the Devices to Achieve Near 100% Triplet Harvesting and High Efficiency. *Adv. Funct. Mater.* **2014**, *24* (39), 6178–6186.
- (22) Pander, P.; Kudelko, A.; Brzeczek, A.; Wroblewska, M.; Walczak, K.; Data, P. Analysis of Exciplex Emitters. *Display Imaging* **2017**, *2*, 265–277.
- (23) Kim, K.-H.; Yoo, S.-J.; Kim, J.-J. Boosting Triplet Harvest by Reducing Nonradiative Transition of Exciplex toward Fluorescent Organic Light-Emitting Diodes with 100% Internal Quantum Efficiency. *Chem. Mater.* **2016**, *28* (6), 1936–1941.
- (24) Cherpak, V.; Stakhira, P.; Minaev, B.; Baryshnikov, G.; Stromlyo, E.; Helzhynskyy, I.; Chapran, M.; Volyniuk, D.; Hotra, Z.; Dabulienė, A.; Tomkeviciene, A.; Voznyak, L.; Grazulevicius, J. V. Mixing of Phosphorescent and Exciplex Emission in Efficient Organic Electroluminescent Devices. *ACS Appl. Mater. Interfaces* **2015**, *7* (2), 1219–1225.
- (25) Wang, M.; Huang, Y.; Lin, K.; Yeh, T.; Duan, J.; Ko, T.; Liu, S.; Wong, K.; Hu, B. Revealing the Cooperative Relationship between Spin, Energy, and Polarization Parameters toward Developing High-Efficiency Exciplex Light-Emitting Diodes. *Adv. Mater.* **2019**, *31* (46), 1904114.
- (26) Zhang, M.; Liu, W.; Zheng, C.; Wang, K.; Shi, Y.; Li, X.; Lin, H.; Tao, S.; Zhang, X. Tricomponent Exciplex Emitter Realizing over 20% External Quantum Efficiency in Organic Light-Emitting Diode with Multiple Reverse Intersystem Crossing Channels. *Adv. Sci.* **2019**, *6* (14), 1801938.
- (27) Nguyen, T. B.; Nakanotani, H.; Hatakeyama, T.; Adachi, C. The Role of Reverse Intersystem Crossing Using a TADF-Type Acceptor Molecule on the Device Stability of Exciplex-Based Organic Light-Emitting Diodes. *Adv. Mater.* **2020**, *32* (9), 1906614.
- (28) Dias, F. B.; Santos, J.; Graves, D. R.; Data, P.; Nobuyasu, R. S.; Fox, M. A.; Batsanov, A. S.; Palmeira, T.; Berberan-Santos, M. N.; Bryce, M. R.; Monkman, A. P. The Role of Local Triplet Excited States and D-A Relative Orientation in Thermally Activated Delayed Fluorescence: Photophysics and Devices. *Adv. Sci.* **2016**, *3* (12), 1600080.
- (29) Etherington, M. K.; Franchello, F.; Gibson, J.; Northey, T.; Santos, J.; Ward, J. S.; Higginbotham, H. F.; Data, P.; Kurowska, A.; Dos Santos, P. L.; Graves, D. R.; Batsanov, A. S.; Dias, F. B.; Bryce, M. R.; Penfold, T. J.; Monkman, A. P. Regio- and Conformational Isomerization Critical to Design of Efficient Thermally-Activated Delayed Fluorescence Emitters. *Nat. Commun.* **2017**, *8*, 14987.
- (30) Marian, C. M. Mechanism of the Triplet-to-Singlet Upconversion in the Assistant Dopant ACRXTN. *J. Phys. Chem. C* **2016**, *120* (7), 3715–3721.
- (31) Glowacki, I.; Szamel, Z. The Nature of Trapping Sites and Recombination Centres in PVK and PVK–PBD Electroluminescent Matrices Seen by Spectrally Resolved Thermoluminescence. *J. Phys. D. Appl. Phys.* **2010**, *43* (29), 295101.

- (32) Glowacki, I.; Szamel, Z. The Impact of 1 Wt% of Ir(Ppy) 3 on Trapping Sites and Radiative Recombination Centres in PVK and PVK/PBD Blend Seen by Thermoluminescence. *Org. Electron.* **2015**, *24*, 288–296.
- (33) Kalinowski, J.; Cocchi, M.; Virgili, D.; Fattori, V.; Williams, J. A. G. Mixing of Excimer and Exciplex Emission: A New Way to Improve White Light Emitting Organic Electrophosphorescent Diodes. *Adv. Mater.* **2007**, *19* (22), 4000–4005.
- (34) *The Exciplex*; Gordon, M., Ware, W. R., Eds.; Academic Press, 1975.
- (35) Lee, D. R.; Kim, M.; Jeon, S. K.; Hwang, S.; Lee, C. W.; Lee, J. Y. Design Strategy for 25% External Quantum Efficiency in Green and Blue Thermally Activated Delayed Fluorescent Devices. *Adv. Mater.* **2015**, *27* (39), 5861–5867.
- (36) Zhang, D.; Cai, M.; Zhang, Y.; Bin, Z.; Zhang, D.; Duan, L. Simultaneous Enhancement of Efficiency and Stability of Phosphorescent OLEDs Based on Efficient Forster Energy Transfer from Interface Exciplex. *ACS Appl. Mater. Interfaces* **2016**, *8* (6), 3825–3832.
- (37) Hung, W.-Y.; Chiang, P.-Y.; Lin, S.-W.; Tang, W.-C.; Chen, Y.-T.; Liu, S.-H.; Chou, P.-T.; Hung, Y.-T.; Wong, K.-T. Balance the Carrier Mobility To Achieve High Performance Exciplex OLED Using a Triazine-Based Acceptor. *ACS Appl. Mater. Interfaces* **2016**, *8* (7), 4811–4818.
- (38) Su, S.-J.; Sasabe, H.; Pu, Y.-J.; Nakayama, K.; Kido, J. Tuning Energy Levels of Electron-Transport Materials by Nitrogen Orientation for Electrophosphorescent Devices with an ‘Ideal’ Operating Voltage. *Adv. Mater.* **2010**, *22* (30), 3311–3316.
- (39) Zhang, L.; Cai, C.; Li, K. F.; Tam, H. L.; Chan, K. L.; Cheah, K. W. Efficient Organic Light-Emitting Diode through Triplet Exciton Reharvesting by Employing Blended Electron Donor and Acceptor as the Emissive Layer. *ACS Appl. Mater. Interfaces* **2015**, *7* (45), 24983–24986.
- (40) Cocchi, M.; Virgili, D.; Sabatini, C.; Kalinowski, J. Organic Electroluminescence from Singlet and Triplet Exciplexes: Exciplex Electrophosphorescent Diode. *Chem. Phys. Lett.* **2006**, *421* (4–6), 351–355.
- (41) Chapran, M.; Pander, P.; Vasylieva, M.; Wiosna-Salyga, G.; Ulanski, J.; Dias, F. B.; Data, P. Realizing 20% External Quantum Efficiency in Electroluminescence with Efficient Thermally Activated Delayed Fluorescence from an Exciplex. *ACS Appl. Mater. Interfaces* **2019**, *11* (14), 13460–13471.
- (42) Dias, F. B.; Bourdakos, K. N.; Jankus, V.; Moss, K. C.; Kamtekar, K. T.; Bhalla, V.; Santos, J.; Bryce, M. R.; Monkman, A. P. Triplet Harvesting with 100% Efficiency by Way of Thermally Activated Delayed Fluorescence in Charge Transfer OLED Emitters. *Adv. Mater.* **2013**, *25* (27), 3707–3714.
- (43) Kalinowski, J.; Cocchi, M.; Virgili, D.; Sabatini, C. Charge Photogeneration Effect on the Exciplex Emission from Thin Organic Films. *Appl. Phys. Lett.* **2006**, *89* (1), No. 011105.
- (44) Kalinowski, J. *Organic Light-Emitting Diodes*; CRC Press, 2018.
- (45) Graves, D.; Jankus, V.; Dias, F. B.; Monkman, A. Photophysical Investigation of the Thermally Activated Delayed Emission from Films of M-MTDATA:PBD Exciplex. *Adv. Funct. Mater.* **2014**, *24* (16), 2343–2351.
- (46) Montanaro, S.; Pander, P.; Mistry, J.-R.; Elsegood, M. R. J.; Teat, S. J.; Bond, A. D.; Wright, I. A.; Congrave, D. G.; Etherington, M. K. Simultaneous Enhancement of Thermally Activated Delayed Fluorescence and Photoluminescence Quantum Yield via Homocoupling. *J. Mater. Chem. C* **2022**, *10* (16), 6306–6313.
- (47) Lakowicz, J. R. *Principles of Fluorescence Spectroscopy*; Springer, 2007.
- (48) Jankus, V.; Chiang, C. J.; Dias, F.; Monkman, A. P. Deep Blue Exciplex Organic Light-Emitting Diodes with Enhanced Efficiency; P-Type or E-Type Triplet Conversion to Singlet Excitons? *Adv. Mater.* **2013**, *25* (10), 1455–1459.
- (49) Jankus, V.; Abdullah, K.; Griffiths, G. C.; Al-Attar, H.; Zheng, Y.; Bryce, M. R.; Monkman, A. P. The Role of Exciplex States in Phosphorescent OLEDs with Poly(Vinylcarbazole) (PVK) Host. *Org. Electron.* **2015**, *20*, 97–102.
- (50) Kabe, R.; Adachi, C. Organic Long Persistent Luminescence. *Nature* **2017**, *550* (7676), 384–387.
- (51) Moon, C.-K.; Huh, J.-S.; Kim, J.-M.; Kim, J.-J. Electronic Structure and Emission Process of Excited Charge Transfer States in Solids. *Chem. Mater.* **2018**, *30* (16), 5648–5654.
- (52) Řezáč, J.; Fanfrlík, J.; Salahub, D.; Hobza, P. Semiempirical Quantum Chemical PM6Method Augmented by Dispersion and H-Bonding Correction Terms Reliably Describes Various Types of Noncovalent Complexes. *J. Chem. Theory Comput.* **2009**, *5* (7), 1749–1760.
- (53) Glowacki, I.; Jung, J.; Wiosna-Salyga, G.; Chapran, M.; Luczak, A.; DuPont, B. G. R.; Luszczynska, B.; Ulanski, J. Role of Charge-Carrier Trapping in Organic Optoelectronic Devices. *Display Imaging* **2017**, *2*, 279–319.
- (54) Hosokai, T.; Noda, H.; Nakanotani, H.; Nawata, T.; Nakayama, Y.; Matsuzaki, H.; Adachi, C. Solvent-Dependent Investigation of Carbazole Benzonitrile Derivatives: Does the LE3–CT1 Energy Gap Facilitate Thermally Activated Delayed Fluorescence? *J. Photonics Energy* **2018**, *8* (03), 1.
- (55) Noda, H.; Chen, X.-K.; Nakanotani, H.; Hosokai, T.; Miyajima, M.; Notsuka, N.; Kashima, Y.; Brédas, J.-L.; Adachi, C. Critical Role of Intermediate Electronic States for Spin-Flip Processes in Charge-Transfer-Type Organic Molecules with Multiple Donors and Acceptors. *Nat. Mater.* **2019**, *18* (10), 1084–1090.
- (56) Pander, P.; Data, P.; Dias, F. B. Time-resolved Photophysical Characterization of Triplet-harvesting Organic Compounds at an Oxygen-free Environment Using an iCCD Camera. *J. Vis. Exp.* **2018**, *142*, e56614.
- (57) de Mello, J. C.; Wittmann, H. F.; Friend, R. H. An improved experimental determination of external photoluminescence quantum efficiency. *Adv. Mater.* **1997**, *9*, 230–232.
- (58) Glowacki, I.; Szamel, Z. The nature of trapping sites and recombination centres in PVK and PVK–PBD electroluminescent matrices seen by spectrally resolved thermoluminescence. *J. Phys. D. Appl. Phys.* **2010**, *43*, 295101.
- (59) Glowacki, I.; Szamel, Z. The impact of 1 wt% of Ir(ppy)3 on trapping sites and radiative recombination centres in PVK and PVK/PBD blend seen by thermoluminescence. *Org. Electron.* **2015**, *24*, 288–296.
- (60) Řezáč, J.; Fanfrlík, J.; Salahub, D.; Hobza, P. Semiempirical Quantum Chemical PM6Method Augmented by Dispersion and H-Bonding Correction Terms Reliably Describes Various Types of Noncovalent Complexes. *J. Chem. Theory Comput.* **2009**, *5* (7), 1749–1760.
- (61) Chai, J.-D.; Head-Gordon, M. Systematic optimization of long-range corrected hybrid density functionals. *J. Chem. Phys.* **2008**, *128*, No. 084106.
- (62) Ditchfield, R.; Hehre, W. J.; Pople, J. A. Self-Consistent Molecular-Orbital Methods. IX. An Extended Gaussian-Type Basis for Molecular-Orbital Studies of Organic Molecules. *J. Chem. Phys.* **1971**, *54*, 724–728.
- (63) Frisch, M. J.; Pople, J. A.; Binkley, J. S. Self-consistent molecular orbital methods 2S. Supplementary functions for Gaussian basis sets. *J. Chem. Phys.* **1984**, *80*, 3265–3269.
- (64) Clark, T.; Chandrasekhar, J.; Spitznagel, G. W.; Schleyer, P. V. R. Efficient diffuse function-augmented basis sets for anion calculations. III.† The 3-21+G basis set for first-row elements, Li–F. *J. Comput. Chem.* **1983**, *4*, 294–301.
- (65) Frisch, M. J.; Trucks, G. W.; Schlegel, H. B.; Scuseria, G. E.; Robb, M. A.; Cheeseman, J. R.; Scalmani, G.; Barone, V.; Petersson, G. A.; Nakatsuji, H.; et al. *Gaussian 16*, revision C.01; Gaussian, Inc.: Wallingford, CT, 2016.
- (66) de Sá Pereira, D.; Data, P.; Monkman, A. P. Methods of Analysis of Organic Light Emitting Diodes. *Display Imaging* **2017**, *2*, 323–337.